



Research

Cite this article: Leigh SC, Summers AP, Hoffmann SL, German DP. 2021 Shark spiral intestines may operate as Tesla valves. *Proc. R. Soc. B* **288**: 20211359. <https://doi.org/10.1098/rspb.2021.1359>

Received: 14 June 2021

Accepted: 30 June 2021

Subject Category:

Morphology and biomechanics

Subject Areas:

bioengineering, physiology, evolution

Keywords:

digestive morphology, CT scan, spiral intestine, Tesla valve, bioinspired design

Author for correspondence:

Samantha C. Leigh

e-mail: scleigh19@gmail.com

Electronic supplementary material is available online at <https://doi.org/10.6084/m9.figshare.c.5508022>.

Shark spiral intestines may operate as Tesla valves

Samantha C. Leigh¹, Adam P. Summers², Sarah L. Hoffmann³
and Donovan P. German⁴

¹Department of Biology, California State University Dominguez Hills, Carson, CA 90747, USA

²Biology and School of Aquatic and Fisheries Sciences, University of Washington, Friday Harbor, WA 98250, USA

³Applied Biological Services, Biomark Inc., Boise, ID 83702, USA

⁴Department of Ecology and Evolutionary Biology, University of California, Irvine, CA, 92617, USA

id SCL, 0000-0001-8675-1259; APS, 0000-0003-1930-9748; SLH, 0000-0003-3376-0121; DPG, 0000-0002-7916-6569

Looking to nature for inspiration has led to many diverse technological advances. The spiral valve intestine of sharks has provided the opportunity to observe the efficiency of different valve systems. It is supposed that the spiral intestine present in sharks, skates and rays slows the transit rate of digesta through the gut and provides increased surface area for the absorption of nutrients. In this investigation, we use a novel technique—creating three-dimensional reconstructions from CT scans of spiral intestines—to describe the morphology of the spiral intestine of at least one species from 22 different shark families. We discuss the morphological data in an evolutionary, dietary and functional context. The evolutionary analyses suggest that the columnar morphology is the ancestral form of the spiral intestine. Dietary analyses reveal no correlation between diet type and spiral intestine morphology. Flow rate was slowed significantly more when the two funnel-shaped spiral intestines were subjected to flow in the posterior to anterior direction, indicating their success at producing unidirectional flow, similar to a Tesla valve. These data are available to generate additional three-dimensional morphometrics, create computational models of the intestine, as well as to further explore the function of the gastrointestinal tract of sharks in structural and physiological contexts.

1. Background

Scientists often turn to nature in search of inspiration when developing new materials and products. This has led to the development of many technological advances such as non-clogging filters inspired by manta ray feeding apparatus [1], adhesives inspired by the northern clingfish [2], robotics inspired by spider silk [3] and countless more. Sometimes, in order to progress towards the future, we need to dig into the past, and in this case, we explore the function of the spiral intestine in elasmobranchs (sharks, skates and rays). Sharks are one of the oldest and most diverse groups of upper trophic level consumers in the ocean [4–6]. They are critical to maintaining the biodiversity of lower trophic levels on which humans rely for food and economic resources [7]. Elasmobranchs consume a broad range of diets (smaller sharks, marine mammals, teleosts, crustaceans, zooplankton, seagrass, etc.; [8]) and are also known for eating large meals on an infrequent basis, potentially going even weeks without a meal [9–11]. The spiral intestine (sometimes referred to as spiral valves; figure 1), effectively expands the surface area and volume of the intestine relative to a straight gut, allegedly increasing gut residence time and nutrient absorption [12–17]. Yet, this gut morphology appears to be restricted to elasmobranchs, with a few exceptions such as Acipenseridae, Dipnoi and Lepisosteidae [8,18–20].

The spiral intestine is located posterior to the stomach and proximal intestine, and anterior to the rectum (figure 1). It consists of a varying number of intestinal tissue folds (2–50) and has been observed in four main morphological

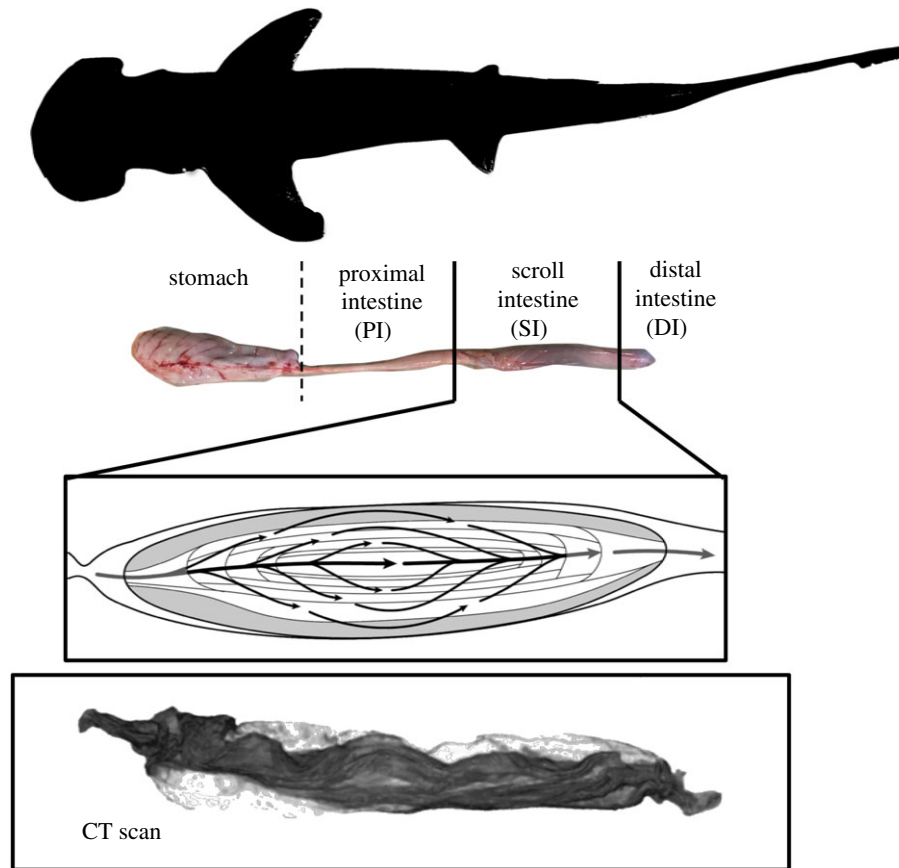


Figure 1. Digestive anatomy of the bonnethead shark (*Sphyrna tiburo*). Drawing of scroll intestine by A. Dingeldein. CT scan reconstruction of scroll intestine by S. Leigh. (Online version in colour.)

forms: columnar, scroll, funnels oriented posteriorly and funnels oriented anteriorly (figure 2) [12,22]. These morphologies have been depicted either as splayed out dissections or as representative two-dimensional slices through the three-dimensional structure (figure 2; originally from [21], reproduced in [12,22,23]). Neither of these provides an adequate understanding of the structures as they reside in the intestine or how they may aid in the control of digesta flow. A recent reconstruction of three-dimensional data from histological sections from a species of cat shark offers a tantalizing glimpse of the anatomy of a scroll-type spiral intestine [24].

Here, we present the three-dimensional morphology of the spiral intestine from 22 families of shark species using X-ray-computed tomography (CT scans; table 1 and figure 3). We tested the hypothesis that the spiral intestine structures may passively (i.e. without any muscular contractions) affect digesta flow, favouring an anterior to posterior flow axis, and preventing back flow (figure 4). That is, spiral intestines may act as naturally occurring Tesla valves (figure 5), preventing backflow without flapper or constrictive valving, and therefore encouraging unidirectional flow. To test this, we measured flow rate through fixed spiral intestines of shark species that represent each of the four morphological forms—columnar, scroll, funnels pointed posteriorly and funnels pointed anteriorly (figure 2). Additionally, because spiral intestines function with muscular contractions in a live organism, we quantified the contraction rate of the intestinal smooth muscle used to transport digesta through *in situ* columnar spiral intestine in recently deceased *Squalus suckleyi* (Pacific spiny dogfish). We also mapped the spiral intestine

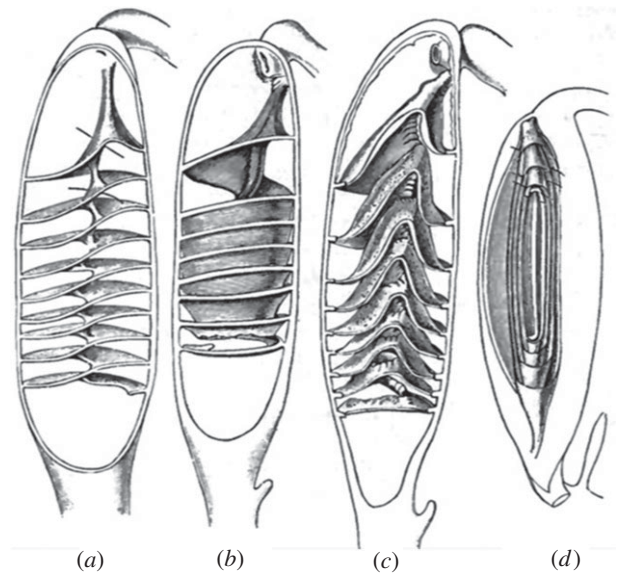


Figure 2. The four spiral intestine structures: (a) columnar, (b) funnels pointed posteriorly, (c) funnels pointed anteriorly and (d) scroll. Adapted from [21].

morphology onto a cladogram to reveal how the diverse spiral intestine structures have evolved and whether the structures correlate with diet. Our aims were to (1) evaluate the movement of material through the spiral intestines using flow rate and intestinal muscle contraction rate, and (2) to compare spiral intestine morphology across shark families and diet types using three-dimensional reconstructions of CT scans.

Table 1. Families, species, spiral intestine shape and diet type for all samples CT scanned. Information regarding shark diet is from [25–31].

family	species	spiral intestine shape	diet
Alopiidae	<i>Alopias vulpinus</i>	column	schooling bony fishes (i.e. menhaden, anchovies)
Carcharhinidae	<i>Carcharhinus leucas</i>	scroll	bony fishes (i.e. skipjack tuna), small elasmobranchs cephalopods, turtles
	<i>Carcharhinus melanopterus</i>	scroll	small bony fishes (i.e. mullet, groupers)
	<i>Carcharhinus amblyrhynchos</i>	scroll	small bony fishes, small elasmobranchs, cephalopods, crustaceans
	<i>Carcharhinus plumeus</i>	scroll	small bony fishes, small elasmobranchs, cephalopods, crustaceans
	<i>Carcharhinus taurus</i>	scroll	small bony fishes, small elasmobranchs, cephalopods, crustaceans
Centrophoridae	<i>Centrophorus granulosus</i> ^a	funnels (anterior)	bony fishes (i.e. mackerels), cephalopods
	<i>Deania calcea</i>	funnels (anterior)	bony fishes (i.e. lanternfishes), cephalopods
Chlamydoselachidae	<i>Chlamydoselachus anguineus</i>	column	small elasmobranchs, cephalopods, bony fishes
Dalatiidae	<i>Squaliolus laticaudus</i>	column	cephalopods, shrimp, bony fishes (i.e. lanternfishes)
Echinorhinidae	<i>Echinorhinus cookei</i>	column	small elasmobranchs, bony fishes, cephalopods
Etmopteridae	<i>Centroscyllium nigrum</i>	funnels (posterior)	bony fishes, variety of invertebrates
Ginglymostomatidae	<i>Ginglymostoma cirratum</i>	funnels (posterior)	molluscs, crustaceans, bony fishes
Hemigaleidae	<i>Chaenogaleus macrostoma</i>	column	small bony fishes, cephalopods, crustaceans
Hemiscylliidae	<i>Hemiscyllium ocellatum</i>	column	polychaete worms, crustaceans
Heterodontidae	<i>Heterodontus francisci</i>	column	benthic invertebrates, small bony fishes
Hexanchidae	<i>Notorynchus cepedianus</i>	scroll	elasmobranchs, marine mammals, bony fishes
Lamnidae	<i>Isurus oxyrinchus</i>	column	bony fishes (i.e. tuna), elasmobranchs, cephalopods
Orectolobidae	<i>Orectolobus maculatus</i>	column	crustaceans, cephalopods, bony fishes
Pseudocarchariidae	<i>Pseudocarcharias kamoharai</i>	scroll	cephalopods, crustaceans, small bony fishes
Scyliorhinidae	<i>Apristurus brunneus</i>	scroll	bony fishes (i.e. lanternfishes), crustaceans
	<i>Cephaloscyllium ventrosum</i> ^a	scroll	benthic molluscs, crustaceans, small bony fishes
Somniosidae	<i>Somniosus pacificus</i>	funnels (anterior)	bony fishes, cephalopods, crustaceans, carrion
Sphyrnidae	<i>Sphyrna lewini</i> ^a	scroll	bony fishes (i.e. sardines), variety of invertebrates
	<i>Sphyrna tiburo</i> ^a	scroll	cephalopods, crustaceans, seagrass
	<i>Sphyrna zygaena</i>	scroll	small elasmobranchs, bony fishes, invertebrates
Squalidae	<i>Squalus acanthias</i>	column	bony fishes (i.e. jack mackerel), cephalopods
	<i>Squalus suckleyi</i> ^a	column	bony fishes (i.e. herring), invertebrates
Squatinae	<i>Squatina dumeril</i>	column	molluscs, crustaceans, fishes (i.e. flounders/stingrays)
Stegostomatidae	<i>Stegostoma fasciatum</i>	column	molluscs, small bony fishes
Triakidae	<i>Mustelus canis</i> ^a	funnels (posterior)	crustaceans, polychaetes, molluscs
	<i>Triakis semifasciata</i>	funnels (posterior)	variety of benthic invertebrates, small bony fishes

^aLyophilized prior to scanning.

2. Material and methods

(a) Specimen collections and CT scanning

Spiral intestines were either dissected from preserved shark specimens (fixed in formalin and stored in an ethanol solution) from the Natural History Museum of Los Angeles County (electronic supplementary material, table S1) or from previously frozen spiral intestines from donated shark specimens. To dissect out the spiral intestine, the ventral body cavity was opened using

a razor blade (from anus to mouth) and cuts with dissecting scissors were made at the distal end of the proximal intestine and the anus. The spiral intestines from all specimens were flushed out with de-ionized water to remove any residual gut contents. They were put through an ethanol series (30%, 50%, 70% in de-ionized water) for a minimum of four hours at each concentration and were stored in 70% ethanol. We stained the intestines in Lugol's solution for a minimum of 4 h. After staining, the intestine was tied off at one end with fishing line, filled with 70%

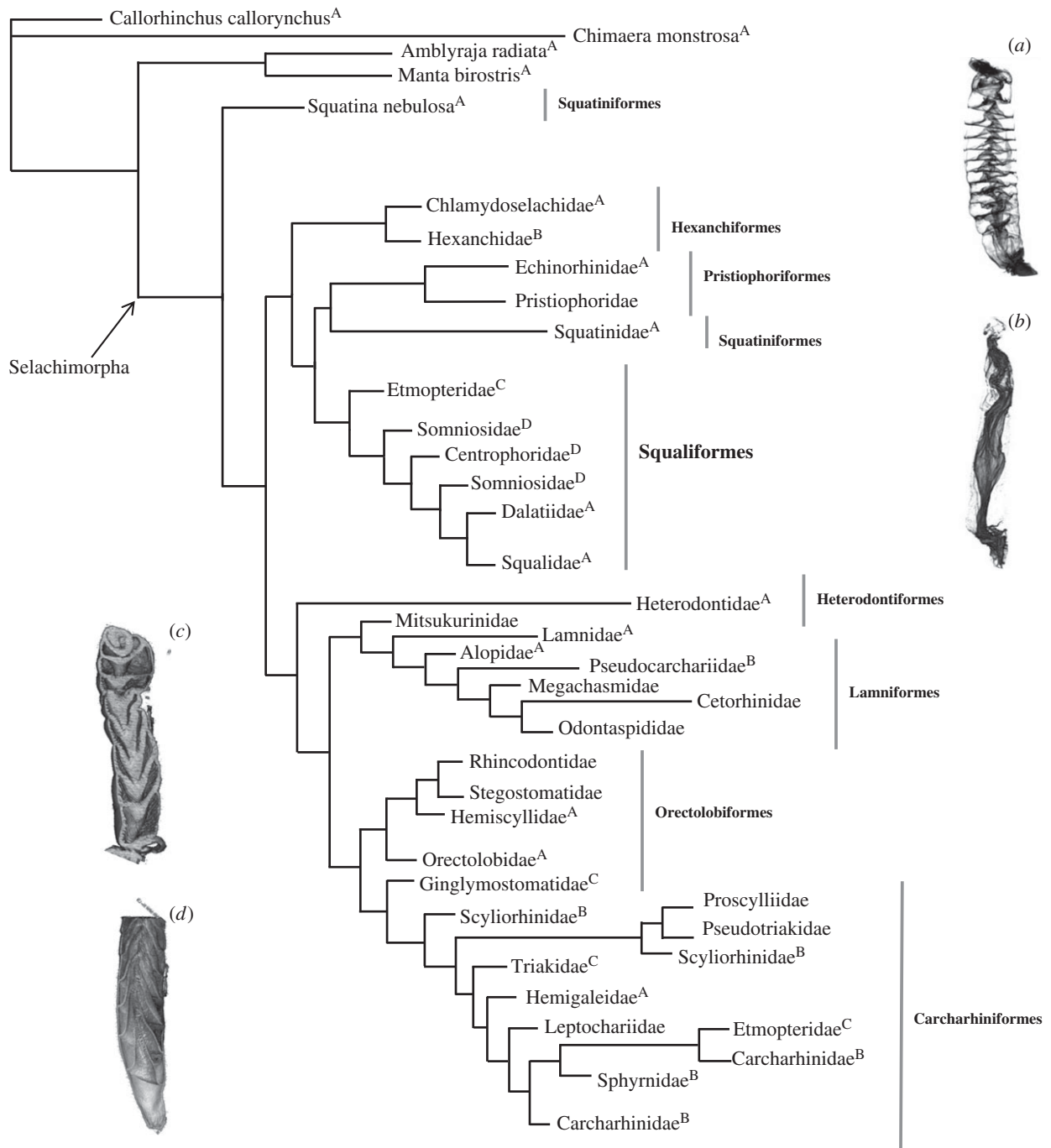


Figure 3. Cladogram of sharks to the family level based on the tree from Vélez-Zuazo & Agnarsson [32] (adapted from Leigh *et al.* [8]), depicting which spiral intestine morphology corresponds to each family. Light grey lines show which families belong to certain orders. (A) Column, (B) scroll, (C) funnels pointed posteriorly and (D) funnels pointed anteriorly. Most basal categories (prior to Selachimorpha) do not have CT scans. Information about spiral intestine structure came from the previous literature.

ethanol, then tied off at the other end with fishing line. They were placed into individually labelled plastic 15 ml or 50 ml vials (depending on the size of the specimen) to be scanned.

CT scanning was done at two different facilities. One set was done at Friday Harbor Laboratories (University of Washington, Friday Harbor, WA, USA). These samples underwent lyophilization (table 1). The lyophilizer (SP Scientific: VerTis, Warminster, PA) was set to -40°C for 2 h prior to use. The caps of the sample vials were loosened and then the vials were placed into the vacuum chamber of the lyophilizer. The vacuum pump was turned on and decreased the pressure in the chamber to 30 millitorr. The samples were left in the vacuum for a minimum of 12 h to ensure complete freeze-drying. At the end of 12 h, the samples were removed from the lyophilizer and kept dry in their individual vials until they could be prepped for CT scanning.

Each sample was removed from its vial and wrapped in dry cheesecloth. All of the cheesecloth-wrapped specimens were then wrapped together as a bundle in more dry cheesecloth. This bundle was placed into a plastic cylinder (size varied based on size of intestine sample) and packed so that no movement of the specimens could occur during the scan. The cylinder was wrapped with plastic wrap and then secured tightly inside the CT scanner (Bruker Skyscan 1173, Kontich, Belgium). The scanner had a 1 mm aluminium filter, and the detector resolution was 1120×1120 voxels ($61.4 \mu\text{m}$ pixels). NRecon (Bruker, Belgium) was used to reconstruct slice images from the projections. After scanning, samples were returned to their individual vials and kept dry. Slice images were further analysed with Data Viewer and CT Vox (both Bruker, Belgium). The files were converted to Dicom format and visualized with Horos

(v. 1.1.7). Each of the spiral intestine types (column, funnel [anterior], funnel [posterior] and scroll) were scanned using this lyophilization method. The remaining spiral intestines were scanned filled with 70% ethanol, which produced highly contrasted images, at University of California (Irvine, CA, USA) using a Gamma Medica X-SPECT scanner (50 kVp, 1000 uA). The image files created by the scan were reconstructed using exxim COBRA (2006 version). This latter set of scanned spiral intestines allowed us to identify the morphological type of each spiral intestine, but the images were not as high-quality as those produced at Friday Harbor Laboratories and were only used for determining spiral shape (either column, scroll, funnel [posterior], or funnel [anterior]).

(b) Flow rate

A 50 l carboy was filled with either 5 l of de-ionized water (dynamic viscosity = 8.9×10^{-4} Pa s), 10% glycerol (dynamic viscosity = 1.3×10^{-3} Pa s), or 25% glycerol (dynamic viscosity = 3×10^{-3} Pa s) in order to represent the variability of viscosities (or resistance to flow) of digesta (depending on the diet type [33]). As a control, a clear plastic tube (15 cm long, 0.75 cm in diameter) was attached to the outflow valve of the carboy and a bucket was placed below the outflow. When the outflow valve was opened, time was recorded until 1 l flowed completely through the clear plastic tubing. This was repeated five times for each of the three viscosities tested. The plastic tubing was removed and replaced with the proximal and spiral intestines (individually) of *Squalus suckleyi* (column), *Centrophorus squamosus* (funnels pointed anteriorly), *Mustelus canis* (funnels pointed posteriorly), and *Sphyrna tiburo* (scroll; all previously fixed overnight in 70% ethanol). These species were chosen to represent each of the four spiral shapes. They were attached (individually) onto the carboy outflow (so water would flow from the anterior end to the posterior end of each intestine), and the process was repeated five times for each intestinal section and each solution viscosity. Flow rate was initially recorded as litres per second and was converted in $\text{m}^3 \text{s}^{-1}$ in order to calculate resistance. Resistance was calculated as the change in pressure divided by flow rate ($R = \Delta P / Q$ [34]). P_1 was calculated as height of the solution column (0.17 m) multiplied by the density of the solution (water: 1000 kg m^{-3} , 10% glycerol: 1023 kg m^{-3} and 25% glycerol: 1062 kg m^{-3}) multiplied by the force of gravity (9.8 m s^{-2} ; $P_1 = h\rho g$). P_2 was determined to be zero since the height of the solution column at P_2 was zero, and therefore, $\Delta P = 0.00166 \text{ MPa}$. Resistance ($\text{MPa} \times \text{s m}^{-3}$) was calculated for the plastic control tube, as well as each proximal intestine and each spiral intestine. Including the length and radius of the intestines was considered for analyses, but digestive tissue is inherently distensible, and therefore accurate and constant measurements of these metrics are difficult to obtain. Furthermore, the existence of the internal spiral intestine structure within this gut region means that different points along the intestine may have different radius measurements and also will add additional overall length to the intestine that cannot be observed from the outside; something that the proximal intestine and the control tubing does not have. To examine whether flow was impeded when moving from the posterior to the anterior end of the intestinal sections, the entire process was repeated with the posterior ends of both the proximal and spiral intestines attached to the carboy outflow so that the flow of water was moving from the posterior end to the anterior end of each intestinal section.

(c) Intestinal smooth muscle contractions

To visualize the smooth muscle contractions of a spiral intestine, five *S. suckleyi* were collected by otter trawl in Friday Harbor, WA. They were transported in live wells to Friday Harbor laboratories on San Juan Island where they were held in two large

round tanks (1 m deep and 2 m in diameter) with flow-through seawater systems (University of Washington IACUC no. 4239-03 to Adam Summers). Contraction experiments were performed on *Squalus suckleyi*. Each shark ($n = 5$) was euthanized using MS-222 in buffered (NaOH) seawater. The shark remained submerged in the MS-222 for 20 min to ensure death. Immediately after death, the ventral body cavity was opened and the proximal and spiral intestines were identified. Corn syrup was mixed with green food colouring (for visibility) to mimic digesta since the corn syrup had a known viscosity (20 poise). A 16-gauge needle attached to a 3 ml syringe was slowly filled to 1 ml with the green corn syrup. The same step was repeated with corn syrup mixed with blue food colouring. The corn syrup with the green food colouring was injected into the lumen of the anterior proximal intestine. The corn syrup with blue food colouring was injected into the lumen of the anterior spiral intestine. In total, 3 ml of 1 M acetylcholine in saline solution (containing 102.7 mM NaCl, 1.61 mM KCl, 1.36 mM CaCl_2 and 1.19 mM NaHCO_3) was injected into the smooth muscle layer of both the anterior proximal and anterior spiral intestine using a 21-gauge needle [35,36]. A timer was started upon the injection of the acetylcholine and a camera (Panasonic Lumix DMC-FZ200) recorded the contractions of the intestines until the food colouring previously injected into the spiral intestine lumen began to emerge from the colon. At this time, the timer was stopped. Throughout this process, seawater was dripped onto the exterior of the intestines using a transfer pipette until the intestines ceased to contract. The video was used to calculate the average number of contractions that occurred per minute, the average length of time (s) that a single contraction took to occur, and to confirm the total time for the dye to pass through the entire length of the spiral intestine. This information was then used to determine the average number of contractions required to move the corn syrup from the anterior of the intestine to the colon. However, the proximal intestine did not contract in response to acetylcholine and therefore the material injected into the proximal intestine never moved through the intestine to the colon. Only the average number of contractions required to move corn syrup through the spiral intestine was calculated.

(d) Statistical analyses

A phylogenetic generalized least-squares (PGLS) test was performed using phylogenetic data from GenBank and the Barcoding of Life Project (as was done by Vélez-Zuazo & Agnarsson [32]) to determine phylogenetic relationships of shark species with respect to their spiral intestine morphology. Correlations between diet and spiral intestine type were determined using a logistic regression test (diets were reduced to numerical categories: 1 = primarily bony fishes; 2 = primarily invertebrates; 3 = marine mammals, elasmobranchs and bony fishes; 4 = bony fishes and invertebrates; 5 = bony fishes, invertebrates and elasmobranchs). This was followed up with an ANOVA ($p < 0.05$) to compare diet type and spiral intestine morphology directly (without considering phylogeny). Comparisons of flow rate were made between proximal and spiral intestines (anteriorly to posteriorly only) for each species using paired t -tests with a Bonferroni-corrected error rate of $p = 0.004$. Comparisons of flow rate among the proximal intestine, the spiral intestine with flow anteriorly to posteriorly and the spiral intestine posteriorly to anteriorly were made using an ANOVA ($p < 0.05$). All statistical analyses were run in R (v. 1.1.383).

3. Results

Volumetric flow rate ($\text{m}^3 \text{s}^{-1}$) measured at two resistances ($\text{MPa} \times \text{s m}^{-3}$) was compared across intestine sample type in all four species (figure 4). The spiral intestines for all species

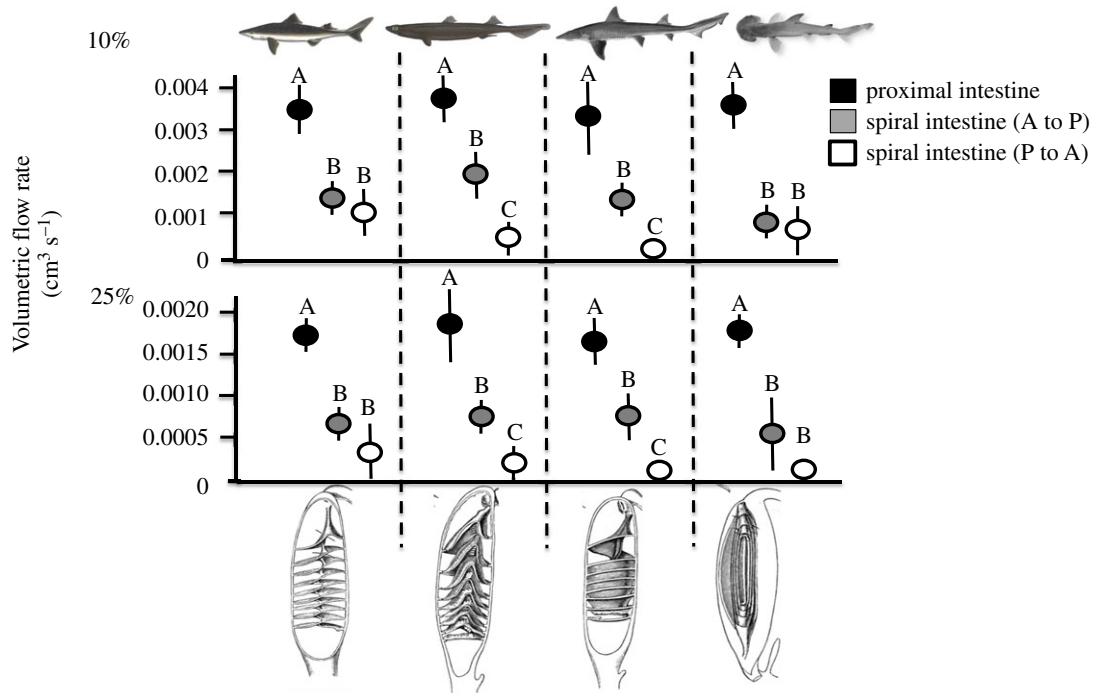


Figure 4. Average volumetric flow rate in the proximal and spiral intestine both oriented anteriorly to posteriorly (A to P) and posteriorly to anteriorly (P to A) for *Squalus suckleyi*, *Centrophorus squamosus*, *Mustelus canis* and *Sphyrna tiburo* using a 10% glycerol solution and 25% glycerol solution. Letters above data points signify significance among intestine sample type for each species (ANOVA, $p < 0.05$).

exhibited a significantly higher resistance and slower volumetric flow rate than the proximal intestines or control tubing for the water ($p < 0.01$), 10% glycerol ($p < 0.05$) and 25% glycerol trials ($p < 0.05$). The control tubing flow rate and resistance was not significantly different from any of the proximal intestines for water ($p = 0.67$), 10% glycerol ($p = 0.43$) or 25% glycerol ($p = 0.31$), showing that the proximal intestine functions as a bore tube. The flow rate of the spiral intestine compared to the proximal intestine as a ratio is three and a half times slower in the spiral intestine than the proximal intestine. Flow rate through the spiral intestines oriented anteriorly/posteriorly was significantly higher than when the intestine was plumbed in reverse for the spiral intestines with the two funnel structures; funnels oriented posteriorly ($p = 0.03$ with water, $p = 0.02$ with 10% glycerol, $p = 0.03$ with 25% glycerol) and anteriorly ($p = 0.01$ with water, $p = 0.01$ with 10% glycerol, $p = 0.02$ with 25% glycerol), but not significantly so for the column ($p = 0.09$ with water, $p = 0.1$ with 10% glycerol, $p = 0.16$ with 25% glycerol) and scroll shapes ($p = 0.11$ with water, $p = 0.2$ with 10% glycerol; $p = 0.14$ with 25% glycerol; figure 4). In other words, there was less resistance to flow in the anterior to posterior direction for the funnel configurations, showing that the structures of the spiral intestine passively engender anterior to posterior flow.

The average number of contractions per minute \pm standard deviation for *S. suckleyi* was 0.7 ± 0.33 . The average amount of time necessary for dyed corn syrup to move from the anterior end of the spiral intestine to the posterior end was 35.6 min (± 13). This was used to calculate the average number of contractions necessary to transport the dyed corn syrup through the spiral intestine, which was 48.2 contractions (± 3.9). The proximal intestine never contracted upon injection of acetylcholine, and never moved the dyed corn syrup through to the spiral intestine.

A full list of the shark species analysed, their spiral intestine morphology types, and their diets can be found in

table 1. There is no significant correlation between diet type and spiral intestine morphology according to the PGLS analysis ($p = 0.4$) and ANOVA ($p = 0.09$). For families with multiple species included in the analyses, different species in a single family tended to have the same spiral intestine morphology; however, different families within a single order can have differing spiral intestine morphologies (figure 3). Generally speaking, the columnar spiral intestine morphology appears ancestral, but other morphologies do not follow a sequence of one morphology (e.g. column) to another (figure 3).

4. Discussion and conclusion

This investigation produced the first three-dimensional renderings of spiral intestines using CT scanning technology, advancing our ability to investigate these structures beyond the two-dimensional histological images and sketches that have been used for the past 130 years (e.g. [14,16,21,22]) and evaluate their effectiveness as valves that generate unidirectional flow. The three-dimensional renderings let us visualize the structure of the tissue folds in the spiral intestine and compare the morphology between species without dissection that disturbs morphology. Additionally, they can be used to quantify the number of intestinal folds, the volume of the lumen and the surface area of gut tissue that may lead to increased levels of nutrient absorption. These three-dimensional renderings let us visualize flow through the spiral intestine and explore the potential uses of these structures when developing mechanical valve systems for industrial purposes. For instance, the spiral intestine of *S. suckleyi* appears to have a central lumen (separate from the spirals), meaning that digesta could pass directly through and bypass the spirals, or travel through the spirals to allow more time for nutrient absorption. The topic of a central lumen in a spiral intestine has not been discussed in the literature, likely

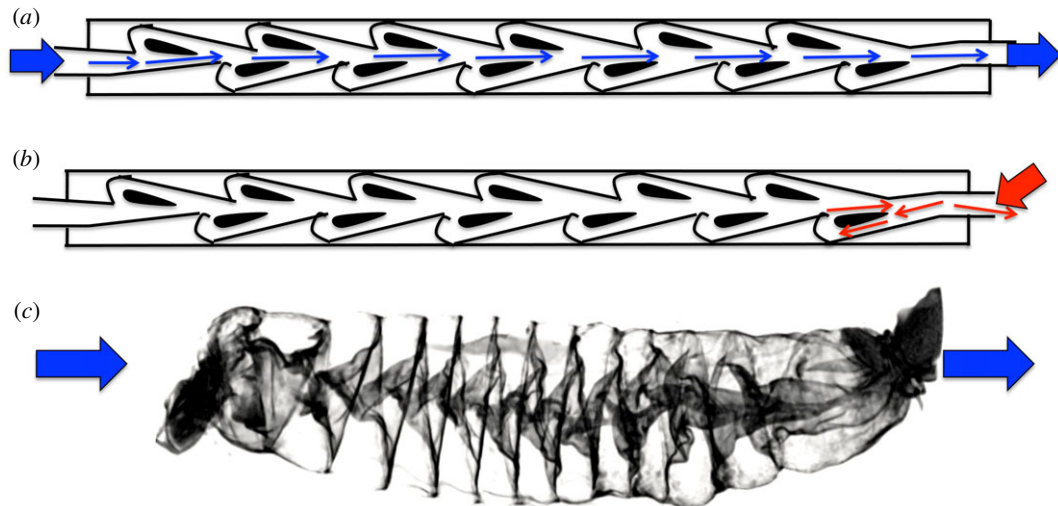


Figure 5. A Tesla valve (*a,b*) produces unidirectional flow without the use of mechanical parts. A spiral intestine (*c*) appears to have a similar structure. (Online version in colour.)

due to the inability to determine the intact shape of a dissected specimen, further demonstrating that these three-dimensional renderings can provide new insights.

We found that a slower flow rate along the posterior to anterior axis is more likely to occur for the two funnel morphologies (figure 4). This suggests that shark families with these funnel morphologies may have slower digesta transit through this intestine region, which could relate to water absorption in the spiral intestine [37]. These observations of flow, combined with the evidence of a central lumen in the column shaped spiral intestine, prompted us to test whether the spiral intestines could function as natural Tesla valves [38]. A Tesla valve allows fluid to move unidirectionally, without any moving parts [39]. Currents flow along different paths and in different directions. These differences have a disproportionate effect on the resistance of the tube (figure 5). The spiral intestine may be working in a similar fashion, which would allow segmental contractions to better mix digesta in the spiral intestine without the risk of much back-flow [33]. Little is known about intestinal motility in sharks. Typically, overall evacuation rate is used to estimate the length of time that digesta remains in the gastrointestinal tract of sharks (i.e. [9]). However, by understanding contractile capabilities of the different segments (proximal, spiral and distal intestines) of the shark digestive system separately, we can begin to establish transit rates at specific points throughout the gut. We have begun to do this by measuring the average number of contractions per minute and the average amount of time necessary to move material of a known viscosity through the spiral intestine of *S. suckleyi*.

Spiral intestines evolved approximately 450 Ma (e.g. [40]; before insects, mammals, birds, etc.), suggesting it is a successful structure in the digestive process. Hence, spiral intestine morphologies should be explored further as mechanisms to produce one-way flow without the use of mechanical parts. While we cannot know the exact morphology of spiral intestines from 450 Ma, there is evidence of fossilized columnar shaped coprolites (e.g. [40]), which provide support for our PGLS analysis that the columnar shape may be the ancestral phenotype (figure 3). There are also some non-elasmobranch fishes that have a spiral intestine such as Acipenseridae (sturgeon [18]), Dipnoi (lungfish [19]) and Lepisosteidae (gar [20]) providing further support that the spiral intestine is a

characteristic that appeared early in the evolution of vertebrates, but also that it has independently evolved in other groups [41]. The roles of these structures in the digestive process should be explored further using *in vivo* investigations.

We confirmed the spiral intestine morphology for species in the majority of shark families. Families within an order do have different spiral structures, though it is common for other morphological features to vary greatly within shark families [42–45]. There is no clear correlation between shark diet types and spiral intestine morphology. For example, *Sphyrna tiburo* has a scroll intestine and consumes a diet consisting of up to 62% (by gut content mass) of seagrass material, along with crustaceans, cephalopods, and small bony fishes [46,47]. However, the closely related *Sphyrna zygaena* also has a scroll intestine, and consumes smaller elasmobranchs, a variety of bony fishes and various invertebrates (e.g. [48]; table 1). There were similar counter-examples to a diet-gut morphology link in other families of sharks where we sampled multiple species (figure 3). The most basal groups (those that arose prior to Selachimorpha) all have columnar spiral intestines, but we see no phylogenetic pattern to the different spiral intestines (figure 3). So, there may well be an underlying functional reason for the different shapes that is not connected to diet. Mapping the spiral intestine onto a cladogram (adapted from [32]) reveals the evolutionary history—with the columnar morphology as ancestral. The scroll intestine is found in the six-gills (Hexanchidae), funnels pointed posteriorly in Etmopteridae and funnels pointed anteriorly in Somniosidae. However, the columnar and scroll intestine morphologies are found in some of the most derived orders, such as the Carcharhiniformes, indicating the structure may play an important functional role.

Investigating the genes involved in spiral intestine development may be crucial in understanding how the different morphologies evolved. For example, roles in gut patterning and subsequent intestinal epithelial and smooth muscle differentiation have been identified for *Hox* genes in *Danio rerio* (zebrafish [49]). Interestingly, genes *Hoxa13* and *Hoxd13* implicate posterior *Hox* gene function during development of the skate spiral intestine [37,50,51]. Furthermore, *pept1* mRNA expression was restricted to the spiral intestine as development progressed for *Scyliorhinus torazame* (cloudy catshark [24]) indicating a possible correlation between an increase in

mRNA expression of *pept1* and the development of the spiral intestine in an oviparous shark *in ovo*. Future investigations should focus on determining if mutations to these genes (*Hoxa13* and *Hoxd13*) or shifts in expression patterns of *pept1* during the developmental process can lead to changes in the morphological development of the spiral intestine in sharks.

In conclusion, our flow rate data suggest that the spiral intestine is acting as a flapper-less Tesla valve, which would promote unidirectional flow without any parts that are susceptible to blockage. We have established, quantitatively, that flow rate is slowed in the spiral intestine. Additionally, the flow rate was slowed significantly more when the two funnel-shaped spiral intestines (anterior and posterior funnels) were subjected to flow in the posterior to anterior direction. This indicates that at least funnel-shaped spiral intestines are capable of producing unidirectional flow, although the spiral and scroll do to a lesser extent. This could explain why digesta transit rates vary among species and among different spiral intestine structures [52–55]. Further investigation of these unique intestinal structures as a component of the digestive success of sharks is necessary to understanding their function and evolution. The new techniques produced by this project lay the groundwork for future investigations involving the spiral intestine, and for understanding the functional role of the digestive tract in sharks, fishes and vertebrates in general.

References

1. Divi RV, Strother J, Paig-Tran EWM. 2018 Manta rays feed using ricochet separation, a novel nondocking filtration mechanism. *Sci. Adv.* **4**, eaat9533. (doi:10.1126/sciadv.aat9533)
2. Ditsche P, Summers A. 2019 Learning from Northern clingfish (*Gobiesox maeandricus*): bioinspired suction cups attach to rough surfaces. *Phil. Trans. R. Soc. B* **374**, 1784. (doi:10.1098/rstb.2019.0204)
3. Pan L *et al.* 2020 A supertough electro-tendon based on spider silk composites. *Nat. Commun.* **11**, 1–9. (doi:10.1038/s41467-020-14988-5)
4. Compagno LJV. 1984 FAO Species Catalogue. Vol. 4. Sharks of the world. An annotated and illustrated catalogue of shark species known to date. Part 2—Carcharhiniformes. *FAO Fish. Synop.* **125**, 251–655. (doi:10.1002/iroh.19870720329)
5. Bucking C. 2015 Feeding and digestion in elasmobranchs: tying diet and physiology together. *Fish Physiol.* **34**, 347–394.
6. Leigh SC, Papastamatiou YP, German DP. 2018 Seagrass digestion by a notorious ‘carnivore’. *Proc. R. Soc. B* **285**, 20181533. (doi:10.1098/rspb.2018.1583)
7. Wetherbee BM, Gruber SH, Cortés E. 1990 Diet, feeding habits, digestion, and consumption in sharks, with special reference to the lemon shark, *Negaprion brevirostris*. *NOAA Technical Report NMFS* **90**, 29–47.
8. Leigh SC, Papastamatiou Y, German DP. 2017 The nutritional physiology of sharks. *Rev. Fish Biol. Fisheries* **27**, 561–585. (doi:10.1007/s11160-017-9481-2)
9. Wetherbee B, Gruber S, Ramsey A. 1987 X-radiographic observations of food passage through digestive tracts of lemon sharks. *Trans. Am. Fish Soc.* **116**, 763–767. (doi:10.1577/1548-8659(1987)116<763:XOOFPT>2.0.CO;2)
10. Cortés E, Papastamatiou YP, Carlson JK, Ferry-Graham L, Wetherbee BM, Cyrino JE, Bureau DP, Kapoor BG. 2008 An overview of the feeding ecology and physiology of elasmobranch fishes. In *Feeding and digestive functions in fishes* (eds J Cyrino, D Bureau, B Kapoor), pp. 393–444. Enfield, NH: Science Publishers.
11. Papastamatiou YP, Watanabe YY, Bradley D, Dee LE, Weng K, Lowe CG, Caselle JE. 2015 Drivers of daily routines in an ectothermic marine predator: hunt warm, rest warmer? *PLoS ONE* **10**, e0127807. (doi:10.1371/journal.pone.0127807)
12. Holmgren S, Nilsson S. 1999 Digestive system. In *Sharks, skates, and rays: the biology of elasmobranch fishes* (ed. WC Hamlett), pp. 144–173. Baltimore, MD: The Johns Hopkins University Press.
13. Chatchavalvanich K *et al.* 2006 Histology of the digestive tract of the freshwater stingray *Himantura signifer* Compagno and Roberts, 1982 (Elasmobranchii, Dasyatidae). *Anat. Embryol.* **211**, 507–518.
14. Theodosiou N, Simeone A. 2012 Evidence of a rudimentary colon in the elasmobranch, *Leucoraja erinacea*. *Dev. Genes Evol.* **222**, 237–243.
15. Jhaveri P, Papastamatiou YP, German DP. 2015 Digestive enzyme activities in the guts of bonnethead sharks (*Sphyrna tiburo*) provide insight into their digestive strategy and evidence for microbial digestion in their hindguts. *Comp. Biochem. Physiol. Part A* **189**, 76–83. (doi:10.1016/j.cbpa.2015.07.013)
16. Dezfuli BS, Manera M, Bosi G, Merella P, Depasquale JA, Giarì L. 2018 Description of epithelial granular cell in catshark spiral intestine: immunohistochemistry and ultrastructure. *J. Morphol.* **280**, 205–213. (doi:10.1002/jmor.20932)
17. Leigh SC, Papastamatiou YP, German DP. 2021 Microbial diversity and function of an omnivorous shark. *Mar. Biol.* **168**, 55. (doi:10.1007/s00227-021-03866-3)
18. Buddington RK, Doroshov SI. 1986 Structural and functional relations of the white sturgeon alimentary canal (*Acipenser transmontanus*). *J. Morphol.* **190**, 201–213. (doi:10.1002/jmor.1051900205)
19. Argyriou T *et al.* Exceptional preservation reveals gastrointestinal anatomy and evolution in early actinopterygian fishes. *Sci. Rep.* **6**, 18758. (doi:10.1038/srep18758)
20. Frias-Quintana CA *et al.* 2015 Development of digestive tract and enzyme activities during the early ontogeny of the tropical gar *Atractosteus tropicus*. *Fish Physiol. Biochem.* **41**, 1–17. (doi:10.1007/s10695-015-0070-9)
21. Parker TJ. 1885 On the intestinal spiral valve in the genus *Raja*. *Zool. Soc. Lond. Trans.* **11**, 49–61.
22. Wilson JM, Castro LFC. 2011 Morphological diversity of the gastrointestinal tract in fishes. In *The multifunctional gut of fish* (eds M Grosell, AP Farrell, CJ Brauner), pp. 1–55. San Diego, CA: Elsevier.
23. Bertin L. 1958 Appareil digestif. In *Traité de zoologie* (ed. PP Grasse), pp. 1248–1302. Paris, France: Mason.
24. Honda Y, Takagi W, Wong MKS, Ogawa N, Tokunaga K, Kofuji K, Hyodo S. 2020 Morphological and

- functional development of the spiral intestine in cloudy catshark (*Scyliorhinus torazame*). *J. Exp. Biol.* **223**, jeb225557. (doi:10.1242/jeb.225557)
25. Compagno L, Dando M, Fowler S. 2005 *Sharks of the world*. Princeton, NJ: Princeton University Press.
 26. Estupiñán-Montaño C, Estupiñán-ortiz JF, Cedeño-figueroa LG, Magaña FG, Polo-Silva CJ. 2017 Diet of the bull shark, *Carcharhinus leucas*, and the tiger shark, *Galeocerdo cuvier*, in the eastern Pacific Ocean. *Turkish J. Zool.* **47**, 1111–1117. (10.3906/zoo-1610-31)
 27. Gelsleichter J, Musick JA, Nichols S. 1999 Food habits of the smooth dogfish, *Mustelus canis*, dusky shark, *Carcharhinus obscurus*, Atlantic sharpnose shark, *Rhizoprionodon terraenovae*, and the sand tiger, *Carcharias taurus*, from the northwest Atlantic Ocean. *Environ. Biol. Fishes* **54**, 205–217. (doi:10.1023/A:1007527111292)
 28. McEroy WD, Wetherbee BM, Mostello CS, Lowe CG, Crow GL, Wass RC. 2006 Food habits and ontogenetic changes in the diet of the sandbar shark, *Carcharhinus plumbeus*, in Hawaii. *Environ. Biol. Fishes* **76**, 81–92. (doi:10.1007/s10641-006-9010-y)
 29. Megalofonou P, Chatzispayrou A. 2006 Sexual maturity and feeding of the gulper shark, *Centrophorus granulosus*, from the eastern Mediterranean Sea. *Cybius: Int. J. Ichthyol.* **30**, 67–74.
 30. Preti A, Smith S, Ramon RD. 2004 *Diet differences in the thresher shark (Alopias vulpinus) during transition from a warm-water regime to a coolwater regime off California-Oregon, 1998–2000*. La Jolla, CA: California Cooperative Oceanic Fisheries Investigations.
 31. Wetherbee BM, Crow GL, Lowe CG. 1997 Distribution, reproduction and diet of the gray reef shark *Carcharhinus amblyrhynchos* in Hawaii. *Mar. Ecol. Progress Series* **151**, 181–189. (doi:10.3354/meps151181)
 32. Vélez-Zuazo X, Agnarsson I. 2011 Shark tales: a molecular species-level phylogeny of sharks (Selachimorpha, Chondrichthyes). *Mol Phylogenet Evol.* **58**, 207–217. (doi:10.1016/j.ympev.2010.11.018)
 33. Lentle RG, Janssen PWM. 2008 Physical characteristics of digesta and their influence on flow and mixing in the mammalian intestine: a review. *J. Comp. Physiol. B* **178**, 673–690. (doi:10.1007/s00360-008-0264-x)
 34. Mearin F, Zacchi P, Arias A, Malagelada J. 1990 Quantification of resistance to flow at the esophagogastric junction in man. *J. Gastrointestinal Motility* **2**, 287–295. (doi:10.1111/j.1365-2982.1990.tb00037.x)
 35. Jensen J, Holmgren S. 1985 Neurotransmitters in the intestine of the Atlantic cod, *Gadus morhua*. *Comp. Biochem. Physiol.* **82**, 81–89. (doi:10.1016/0742-8413(85)90213-0)
 36. Kitazawa T, Hoshi T, Chugun A. 1990 Effects of some autonomic drugs and neuropeptides on the mechanical-activity of longitudinal and circular muscle strips isolated from the carp intestinal bulb (*Cyprinus carpio*). *Comp. Biochem. Physiol. C-Pharmacol. Toxicol. Endocrinol.* **97**, 13–24. (doi:10.1016/0742-8413(90)90165-6)
 37. Theodosiou N, Simeone A. 2012 Evidence of a rudimentary colon in the elasmobranch, *Leucoraja erinacea*. *Dev. Genes Evol.* **222**, 237–243. (doi:10.1007/s00427-012-0406-8)
 38. Cieri R, Farmer CG. 2016 Unidirectional pulmonary airflow in vertebrates: structure, function, evolution. *Comparative Biochemistry and Physiology B* **186**, 541–552. (doi:10.1007/s00360-016-0983-3)
 39. Nobakht A, Shahsavan M, Paykani A. 2013 Numerical study of diodicity mechanism in different tesla-type microvalves. *J. Appl. Res. Technol.* **11**, 876–885. (doi:10.1016/S1665-6423(13)71594-3)
 40. Williams ME. 1972 The origin of ‘spiral coprolites’. *The University of Kansas Paleontological Contributions* **59**, 1–19.
 41. Kikugawa K, Katoh K, Kuraku S, Sakurai H, Ishida O, Iwabe N, Miyata T. 2004 Basal jawed vertebrate phylogeny inferred from multiple nuclear DNA-coded genes. *BMC Biol.* **2**, 3. (doi:10.1186/1741-7007-2-3)
 42. Mara KR. 2010 Evolution of the hammerhead cephalofoil: shape change, space utilization, and feeding biomechanics in hammerhead sharks (Sphyrnidae). Graduate School Thesis, University of Florida.
 43. Mollen FH, Wintner S, Iglesias S, Van Sommeran S, Jagt J. 2012 Comparative morphology of rostral cartilages in extant mackerel sharks (Chondrichthyes, Lamniformes, Lamnidae) using CT scanning. *Zootaxa* **3340**, 29–43. (doi:10.11646/zootaxa.3340.1.2)
 44. Irschick DJ, Fu A, Lauder G, Wilga C, Kuo C-Y, Hammerschlag N. 2017 A comparative morphological analysis of body and fin shape for eight shark species. *Biol. J. Linnean Soc.* **122**, 589–604. (doi:10.1093/biolinnean/blx088)
 45. Hoffmann SL, Buser T, Porter ME. 2020 Comparative morphology of shark pectoral fins. *J. Morphol.* **281**, 1501–1516. (doi:10.1002/jmor.21269)
 46. Cortés E, Charles M, Hueter R. 1996 Diet, feeding habits, and diel feeding chronology of the bonnethead shark, *Sphyrna tiburo*, in Southwest Florida. *Bull. Mar. Sci.* **58**, 353–367.
 47. Bethea DM *et al.* 2007 Geographic and ontogenetic variation in the diet and daily ration of the bonnethead shark, *Sphyrna tiburo*, from the eastern Gulf of Mexico. *Mar. Biol.* **152**, 1009–1020. (doi:10.1007/s00227-007-0728-7)
 48. Smale MJ, Cliff G. 1998 Cephalopods in the diets of four shark species (*Galeocerdo cuvier*, *Sphyrna lewini*, *S. zygaena* and *S. mokarran*) from KwaZulu-Natal, South Africa. *South African J. Mar. Sci.* **20**, 241–253. (doi:10.2989/025776198784126610)
 49. Wallace KN *et al.* 2005 Intestinal growth and differentiation in zebrafish. *Mech. Dev.* **122**, 157–173.
 50. Theodosiou NA, Hall DA, Jowdry AL. 2007 Comparison of acidmucin goblet cell distribution and Hox13 expression patterns in the developing vertebrate digestive tract. *J. Exp. Zool. B Mol. Dev. Evol.* **308**, 442–453.
 51. Warot X, Fromental-Ramain C, Fraulob V, Chambon P, Dolle P. 1997 Gene dosage-dependent effects of the Hoxa13 and Hoxd13 mutations on morphogenesis of the terminal parts of the digestive and urogenital tracts. *Development* **124**, 4781–4791.
 52. Aedo G, Arancibia H. 2001 Gastric evacuation of the redspotted catshark under laboratory conditions. *J. Fish Biol.* **58**, 1454–1457. (doi:10.1111/j.1095-8649.2001.tb02299.x)
 53. Bush A, Holland K. 2002 Food limitation in a nursery area: estimates of daily ration in juvenile scalloped hammerheads, *Sphyrna lewini* (Griffith and Smith, 1834) in Kane’ohe Bay, O’ahu, Hawai’i. *J. Exp. Mar. Biol. Ecol.* **278**, 157–178. (doi:10.1016/S0022-0981(02)00332-5)
 54. Papastamatiou YP, Lowe CG. 2004 Postprandial response of gastric pH in leopard sharks (*Triakis semifasciata*) and its use to study foraging ecology. *J. Exp. Biol.* **207**, 225–232. (doi:10.1242/jeb.00741)
 55. Papastamatiou YP, Purkis SJ, Holland KN. 2007 The response of gastric pH and motility to fasting and feeding in free swimming blacktip reef sharks, *Carcharhinus melanopterus*. *J. Exp. Mar. Biol. Ecol.* **345**, 129–140. (doi:10.1016/j.jembe.2007.02.006)